

Topological phononic crystal

Zhaoju Yang¹, Fei Gao¹, Xiao Lin¹, Yidong Chong^{1,2} and Baile Zhang^{1,2*}

¹*Division of Physics and Applied Physics, School of Physical and Mathematical Sciences,
Nanyang Technological University, Singapore 637371, Singapore.*

²*Centre for Disruptive Photonic Technologies,
Nanyang Technological University, Singapore 637371, Singapore.*

**To whom correspondence should be addressed:*

E-mail: blzhang@ntu.edu.sg.

Abstract

The concept of topologically nontrivial bandstructures, which originally arose in the study of the quantum Hall effect and topological insulator materials, has recently led to the emergence of the field of “topological photonics”. Here, we further extend the concept to acoustics by designing a phononic crystal which maps theoretically onto the integer quantum Hall effect. Time-reversal symmetry is broken by a circulating fluid flow in each unit cell, which corresponds to nonzero periodic effective magnetic flux density. We derive the bandstructure, and show the existence of topologically nontrivial bands possessing nonzero Chern numbers. Numerical simulations reveal the existence of unidirectional acoustic modes at the boundaries of the phononic crystal, which are topologically protected against backscattering from disorder. Such topological phononic crystals may have novel applications in acoustics.

The recent emergence of the field of topological photonics [1] has shown that it is possible to realize classical systems that mimic the exotic quantum materials known as topological insulators. The most striking property of these photonic devices is the existence of “topologically-protected” electromagnetic states, which propagate in a single direction along an edge and are robust against backscattering from disorder [2-4]. This phenomenon relies on the presence of a photonic bandstructure that is “topologically nontrivial”, i.e., not smoothly deformable into the bandstructure of a conventional photonic crystal. The concept of topologically distinct bandstructures first arose in condensed matter physics, in systems now collectively referred to as “topological insulators” [5, 6]; the earliest and most simple examples of these are integer quantum Hall systems, which are non-interacting two-dimensional (2D) electron gases subject to external magnetic fields. It was Haldane and Raghu who pointed out that topologically nontrivial bandstructures need not be limited to fermionic systems, but can equally well arise in bosonic systems, such as photonic crystals with broken time-reversal symmetry [2]. Soon afterwards, the concept was realized experimentally in a microwave-scale magneto-optic photonic crystal [3, 4]. Subsequently, a variety of other “topological photonics” devices have been proposed or demonstrated, with operating frequencies ranging from microwave to optical scales [7-12].

Phononic crystals (PCs) are acoustic devices with close historical and conceptual ties to photonic crystals. They are formed by materials with acoustic properties (elastic moduli and mass densities) that vary periodically in space, on a scale comparable to the acoustic wavelength. Thus far, the PC field has been largely isolated from developments in the field of topological photonics. (There have been a few recent theoretical studies involving topological phonon modes, but these are not closely related [13, 14].) It is the purpose of this Letter to bridge this gap, by proposing and analyzing a PC system with a topologically nontrivial acoustic bandstructure and topologically-protected edge states.

A PC can be formed by a lattice of acoustic “meta-atoms” with subwavelength-scale features [15]. Such systems, which are also called “acoustic metamaterials”, can alter the propagation characteristics of acoustic waves by the formation of an acoustic (or “phononic”) bandstructure. As suggested by Haldane and Raghu in the photonic context, the simplest way to realize a topologically nontrivial bandstructure is to break time-reversal (TR) symmetry, similar to the application of an external magnetic field in quantum Hall systems. Although traditional PCs lack an efficient mechanism for breaking TR symmetry, recent studies indicate that one way to achieve this is to use a circulating fluid. Acoustic “meta-atoms” equipped with circulating fluids have been shown to exhibit giant for acoustic waves [16, 17], and this principle has been used to realize an acoustic circulator device with unprecedented sound isolation properties [17].

We investigate a PC consisting of acoustic “meta-atoms” containing circulating fluid. By studying the acoustic master equation in this system, we show that the PC maps formally onto quantum Hall system of zero-energy electron waves in a periodic magnetic field. The bandstructure contains Dirac point degeneracies which are lifted by the presence of the circulating fluid; the resulting acoustic bands have nonzero Chern numbers, indicating that they are topologically nontrivial [2]. Numerical simulations of the acoustic equations reveal existence of one-way edge states at the boundaries of this PC, which are topologically protected against backscattering by disorder.

A schematic of the 2D PC is shown in Fig. 1(a). It consists of a triangular lattice of constant a , where each unit cell consists of a dense solid cylinder (e.g. a metal cylinder) with radius r_1 , surrounded by a cylindrical fluid-filled region of radius r_2 . The remainder of the cell consists of a stationary fluid, separated from the fluid in the cylindrical region by a thin impedance-matched layer at the cylinder's surface. (This layer can be achieved using a thin sheet of solid material that is permeable to sound.) The central cylinder rotates along its axis

with angular speed Ω , which produces a circulatory flow in the surrounding fluid. (We will not consider the possibility of Taylor vortex formation [18] caused by large Ω in experiment because we here focus on 2D model and Taylor vortex contribute an effective flux in x-y plane.) We assume that fluid velocity is much slower than the speed of sound (Mach number of less than 0.3). The motion of the fluid can be described by a circulating "Couette flow" distribution [18]; the velocity field points in the azimuthal direction, with component v_θ , where r is measured from the origin at the axis of the cylinder. This velocity is equal to

$$v_\theta = -\frac{\Omega r_1^2}{r_2^2 - r_1^2} r + \frac{\Omega r_1^2 r_2^2}{r_2^2 - r_1^2} \frac{1}{r}.$$

The propagation of acoustic waves in the presence of such a steady-state non-homogenous velocity "background" is described in Refs. [19, 20]. Assuming that the viscosity and heat flow are negligible, the waves obey an "acoustic master equation"

$$\frac{1}{\rho} \nabla \cdot \rho \nabla \phi - (\partial_t + \vec{v}_0 \cdot \nabla) \frac{1}{c^2} (\partial_t + \vec{v}_0 \cdot \nabla) \phi = 0 \quad (1)$$

where ρ is the fluid density, c is the speed of sound, and \vec{v}_0 is the background fluid velocity. The relation between the velocity potential ϕ and the acoustic pressure p is given by $p = \rho(\partial_t + \vec{v}_0 \cdot \nabla) \phi$. We model the surface of each cylinder as an impenetrable hard boundary by setting $\vec{n} \cdot \nabla \phi = 0$ along the surface, where \vec{n} is the surface normal vector. We restrict our attentions to time-harmonic solutions with frequency ω and neglect second order terms as $|\vec{v}_0 / c|^2 \ll 1$. With a change of variables $\Psi = \sqrt{\rho} \phi$, the master equation can be rewritten as

$$[(\nabla - i\vec{A}_{eff})^2 + V(x, y)]\Psi = 0 \quad (2)$$

where the effective vector and scalar potentials are

$$\vec{A}_{eff} = -\frac{\omega \vec{v}_0(x, y)}{c^2} \quad (3)$$

$$V(x, y) = -\frac{1}{4} |\nabla \ln \rho|^2 - \frac{1}{2} \nabla^2 \ln \rho + \frac{\omega^2}{c^2} \quad (4)$$

Evidently, Eq. (2) maps onto the Schrodinger equation for a zero-energy electron wavefunction in nonuniform vector and scalar potentials. For nonzero Ω , effective magnetic flux can be given as $\int \vec{A}_{eff} dl$, which indicates the effective magnetic flux in each unit cell decreases with the radius between two cylinders; the net magnetic flux, integrated over the entire unit cell, is zero. Because the effective magnetic flux density is nonzero at various points in the unit cell, TR symmetry is broken. The PC thus behaves like a “zero field quantum Hall” system [21], and is periodic in the unit cell.

It is worth mentioning that a similar approach of using circulating fluids to construct an effective magnetic vector potential for classical wave propagation has been discussed by M. Berry and colleagues [22, 23]. These authors showed that an irrotational (“bathtub”) vortex model of a circulating fluid (e.g., water swirling irrotationally into bathtub vortex) exhibits a classical wavefront dislocation effect which is analogous to the Aharanov-Bohm effect. Here we advance this insight by applying the flow model to a PC context, so that the effective magnetic vector potential gives rise to a topologically nontrivial acoustic bandstructure.

From Eq. (1), we can calculate the acoustic bandstructures of the PC numerically, using the finite element method. For simplicity, we assume the fluids involved are air. The results, with $\Omega = 0$ and $\Omega \neq 0$, are shown in Fig. 1(b). For $\Omega = 0$ [red curves in Fig. 1(b)], the acoustic bandstructure exhibits a pair of Dirac points at the corner of the hexagonal Brillouin zone (BZ), at frequency $\omega_0 = 0.577 \times 2\pi c_a / a$, where c_a is the sound velocity in air; these Dirac points are associated with the spatial inversion and TR symmetries of the lattice.

For $\Omega \neq 0$, the circulating air flow produces a dramatic change in the bandstructure [blue curves in Fig. 1(b)]. Here, we set the angular velocity of the inner rods to be $\Omega = 2\pi \times 400$ rad/s (400 RPS, achievable with miniature electric motors). The Dirac point degeneracies are lifted, producing a finite complete bandgap. The frequency splitting at the zone corners, as a function of the angular velocity Ω , is plotted in Fig. 1(c). This determines

the operational frequency bandwidth of the topological PC. The ratio of the operating frequency to the bandgap, which is an estimate for the penetration depth of the topological edge states in units of the lattice constant, is on the order of 10 for the range of angular velocities plotted here.

Each acoustic band can be characterized by a topological invariant, the Chern number [2]. These can be computed in the usual way; the Berry connection and Chern number of the n th phononic band can be defined as follows:

$$\vec{\mathcal{A}}_n = i \langle \phi_{nk} | \nabla_{\vec{k}} | \phi_{nk} \rangle \quad (5)$$

$$C_n = \frac{1}{2\pi} \iint_{BZ} (dk_a \wedge dk_b) \nabla_{\vec{k}} \times \vec{\mathcal{A}}_n \quad (6)$$

We have numerically verified that the two bands in Fig. 1(b), which are split by the TR breaking, have Chern numbers of ± 1 . The principle of "bulk-edge correspondence" then predicts that, for a finite PC, the gap between these two bands is spanned by unidirectional acoustic edge states, analogous to the electronic edge states occurring in the quantum Hall effect [24].

To confirm the existence of these topologically-protected acoustic edge states, we numerically calculate the bandstructure for a 20×1 super-cell [25], corresponding to a ribbon that is finite (20 unit cells wide) in the y direction and infinite along the x direction. As shown in Fig. 2(a), for $\Omega = 2\pi \times 400$ rad/s the bandgap contains two sets of acoustic edge states, which are confined to opposite edges of the ribbon and have opposite group velocities.

Figs. 2(b) and 2(c) show the propagation of these edge states in a finite (38×10) lattice. In these simulations, the upper edge of the PC is enclosed by a sound-impermeable boundary, in order to prevent the acoustic waves from leaking into the upper half space; absorbing boundary conditions are applied to the sides. A point acoustic source with mid-gap frequency ω_0 is placed near the upper boundary. For $\Omega = 2\pi \times 400$ rad/s, this excites a unidirectional edge state which propagates to the left along the interface, as shown in Fig.

2(b). If the sign of the angular velocity is reversed, the edge state would be directed to the right (not plotted). Fig. 2(c) shows the field distribution for a reduced angular velocity $\Omega = 2\pi \times 200$ rad/s. The reduction in angular velocity leads to a narrow bandgap, which yields an edge state with a longer penetration depth.

Due to the lack of backward-propagating edge modes, the presence of disorder cannot cause backscattering. In Figs. 3(a)-(b), we demonstrate this "topological protection" with two types of interfacial disorder. Fig. 3(a) shows an acoustic cavity located along the interface; the incident wave flows through the cavity, and excites localized resonances within the cavity, but does not backscatter. Fig. 3(b) shows a Z-shape bend connecting two parallel surfaces at different y ; again, the acoustic edge states are fully transmitted across the bend. Finally, Fig. 3(c) shows a 180-degree acoustic bend which allows acoustic edge states to be guided from the top of a sample to the bottom of the sample; note that the left boundary in this sample is a zig-zag boundary, which supports one-way edge states with different dispersion relations.

In summary, we have proposed and analyzed a PC which is formally analogous to a zero-field quantum Hall system, and has a topologically nontrivial acoustic bandstructure. The effective magnetic flux is achieved by circulating fluid flows in each unit cell, which break time-reversal symmetry. We have shown by explicit calculation that the bands have nonzero Chern number, and numerical solutions of the acoustic equations reveal the existence of one-way edge states which are topologically protected against backscattering. Acoustic devices based on these principles may be useful for isolation, noise control, acoustic beam steering, energy harvesting, sensing et al. Our proposed PC design should be quite practical to realize. Similar effects can be achieved with alternative designs featuring circulatory fluid velocity distributions different from the Couette flow studied in this paper; e.g., having azimuthally-directed fans in each unit cell [17], or stirring with a rotating disc on the top plate [26]. We have numerically confirmed that two widely-used velocity distribution models, the

mean flow model [17] and irrotational flow [22, 23], both give rise as well to topologically nontrivial edge states.

This work was sponsored by Nanyang Technological University under Start-Up Grants, and Singapore Ministry of Education under Grant No. Tier 1 RG27/12 and Grant No. MOE2011-T3-1-005. CYD acknowledges support from the Singapore National Research Foundation under grant No. NRFF2012-02.

References

1. L. Lu, J. D. Joannopoulos and M. Soljacic, *Nature Phot.* 8, 821-829 (2014).
2. F. Haldane and S. Raghu, *Phys. Rev. Lett.* 100, 013904 (2008).
3. Z. Wang, Y. Chong, J. D. Joannopoulos and M. Soljacic, *Phys. Rev. Lett.* 100, 13905 (2008).
4. Z. Wang, Y. Chong, J. D. Joannopoulos and M. Soljacic, *Nature* 461, 772-775 (2009).
5. M. Z. Hasan and C. L. Kane, *Rev. Mod. Phys.* 82, 3045–3067 (2010).
6. X. L. Qi and S. C. Zhang, *Rev. Mod. Phys.* 83, 1057–1110 (2011).
7. M. Hafezi, E. A. Demler, M. D. Lukin and J. M. Taylor, *Nature Phys.* 7, 907-912 (2011).
8. Y. Poo, R. X. Wu, Z. F. Lin, Y. Yang and C. T. Chan, *Phys. Rev. Lett.* 106, 093903 (2011).
9. K. Fang, Z. Yu and S. Fan, *Nature Phot.* 6, 782-787 (2012).
10. M. Hafezi, S. Mittal, J. fan, A. Migdall and J. M. Taylor. *Nature Phot.* 7, 1001-1005 (2013).
11. M. C. Rechtsman et al. *Nature* 496, 196-200 (2013).
12. A. B. Khanikaev et al. *Nature Mater.* 12, 233-239 (2012).
13. E. Prodan and C. Prodan, *Phys. Rev. Lett.* 103, 248101 (2009).
14. C. L. Kane and T. C. Lubensky, *Nature Phys.* 10, 39–45 (2013).
15. Z. Y. Liu, et al. *Science* 289, 1734-1736 (2000).
16. P. Roux and M. Fink, *Eur. Lett.* 32 (1), 25-29 (1995).
17. R. Fleury, D. L. Sounas, C. F. Sieck, M. R. Haberman and A. Alu, *Science* 343, 516-519 (2014).
18. P. K. Kundu and I. M. Cohen, *Fluid Mechanics*. (Elsevier, USA, 2012).
19. L. M. Brekhovskikh and O. A. Godin, *Acoustics of Layered Media II: Point Sources and Bounded Beams*. (Springer, Berlin, 1999).
20. A. D. Pierce, *J. Acoust. Soc. Am.* 87, 2292 (1990).
21. F. Haldane, *Phys. Rev. Lett.* 61, 2015 (1988).

22. M. V. Berry, R. G. Chambers, M. D. Large, C. Upstill and J. C. Walmsley, Eur. J. Phys. 1, 154-162 (1980).
23. U. Leonhardt and T. Philbin, Geometry and light: the science of invisibility. (Dover, New York, 2010).
24. Y. Hatsugai, Phys. Rev. Lett. 71, 3697 (1993).
25. J. D. Joannopoulos et al. Photonic crystals: molding the flow of light. (Princeton, New Jersey, 2008).
26. M. Fink, Physics Today 50, 34-40 (1997).

Figure legends

FIG. 1 (color online). Principle of a two-dimensional topological phononic crystal and its band structure. (a) Triangular lattice of the phononic crystal with lattice constant a . Inset shows a Wigner-Seitz unit cell. The central metal rod has radius $r_1 = 0.2a$. Each unit cell is equipped with an anticlockwise circulating fluid flow indicated by little red arrows in the region of radius $r_2 = 0.4a$. (b) Band structures of the phononic crystal without (red curves; $\Omega = 2\pi \times 0$ rad/s) and with (blue curves; $\Omega = 2\pi \times 400$ rad/s) the bias angular velocity. Chern numbers of ± 1 (blue numbers) are labeled for the split bands. Right inset shows the enlarged view of Dirac cone. Left lower inset indicates the first BZ. (c) Frequency splitting as a function of the Revolution Per Second (RPS). The degeneracy at the Dirac point is removed as long as $\Omega \neq 0$.

FIG. 2 (color online). Acoustic one-way edge states. (a) Dispersion of the one-way acoustic edge states (red curves) supported by a finite ribbon of the phononic crystal for $\Omega = 2\pi \times 400$ rad/s. The left and right red curves correspond to the bottom and top edge states, respectively, as indicated by the insets. (b, c) Demonstration of the one-way edge states. The normalized acoustic pressure p for a left-propagating acoustic edge state around frequency $\omega_0 = 0.577 \times 2\pi c_a / a$ for (b) $\Omega = 2\pi \times 400$ rad/s and (c) $\Omega = 2\pi \times 200$ rad/s.

FIG. 3 (color online). Demonstration of the robustness of acoustic one-way edge states against disorders. Topological protection requires the waves to be fully transmitted through (a) an acoustic cavity, (b) a Z-shape bend along the interface, (c) a 180-degree sharp bend with perfect transmission. The operating frequency is around $\omega_0 = 0.577 \times 2\pi c_a / a$ and $\Omega = 2\pi \times 400$ rad/s.

Figure 1

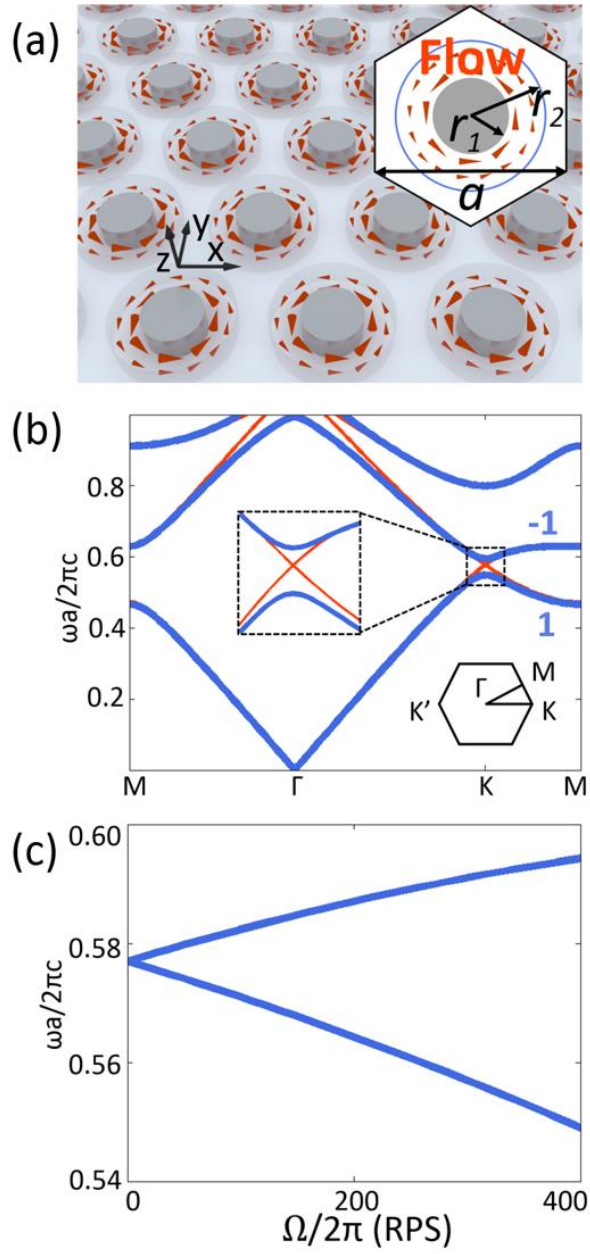


Figure 2

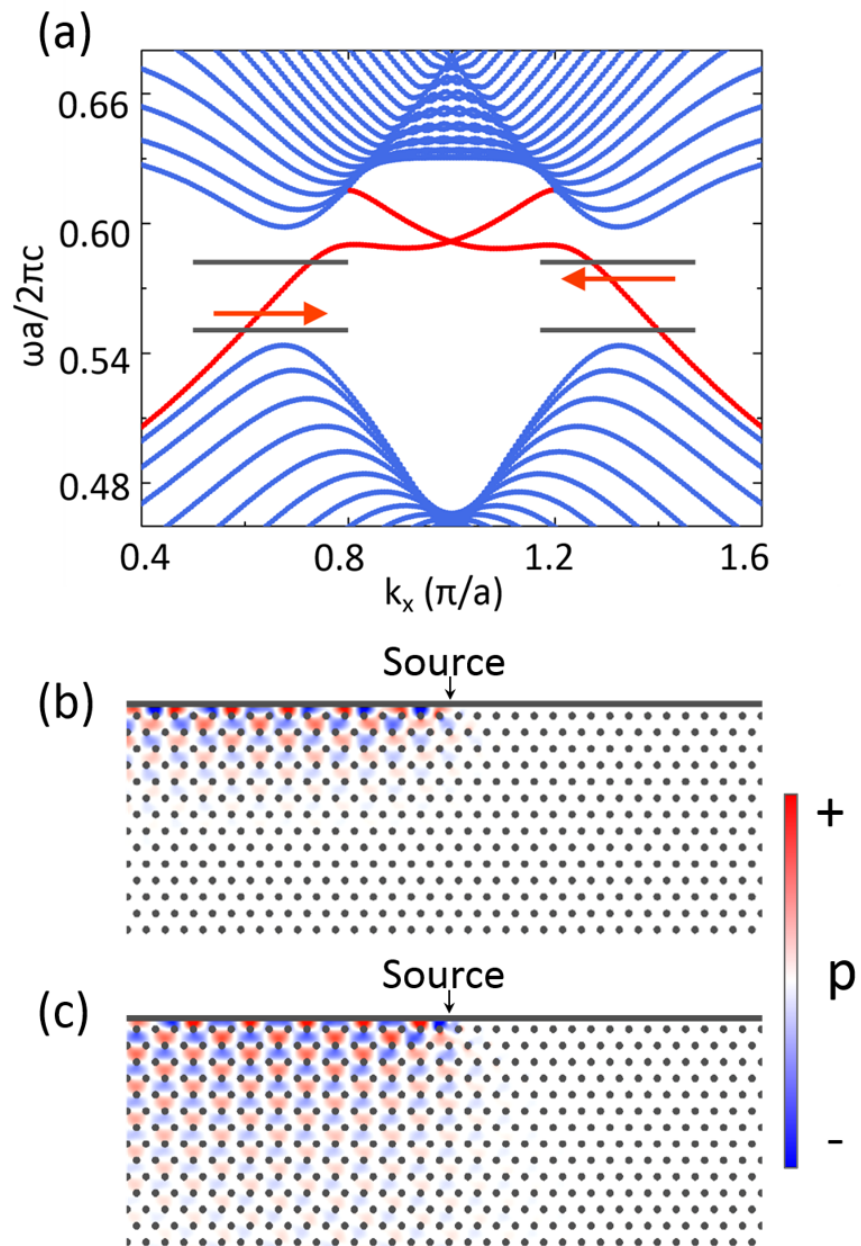


Figure 3

